Climate Dynamics (1992) 8:13-27

Climate Dynamics

A global monthly climatology of soil moisture and water balance

Y Mintz[1,*] **and YV Serafini**[2]

[1] Department of Meteorology, University of Maryland, College Park, MD 20742, and Goddard Laboratory for Atmospheres, NASA/Goddard Space Flight Center, Greenbelt MD 20771, USA
[2] Laboratoire de Météorologie Dynamique du CNRS, Ecole Normale Supérieure, F-75231 Paris Cedex 05, France

Received October 21, 1991/Accepted March 4, 1992

Abstract. Global monthly climatology of available soil moisture content is derived on a 4° by 5° grid from observed precipitation and air surface temperature by use of a simple water budget model. The governing equations and methods of calculation for deriving these fields, which follow the formulation of Thornthwaite, are first described and the importance of the various assumptions and simplifications of this approach are discussed. The derived global fields are then presented. A comparison of some of the derived fields with other calculations is also made in order to permit an evaluation of the results: For example, our indirect estimate of the river run-off is generally in good agreement with more direct estimates, except for high latitude regions where the freezing of the soil may play an important role.

Introduction

The purpose of this paper is to describe a global monthly climatology of soil moisture available for evapotranspiration that was produced some years ago by Mintz and Serafini (1981). These fields of soil moisture were used in a number of published studies (Suarez et al. 1983; Randall 1983; Serafini and Sud 1987). As one of the very few existing data sets of soil moisture it has also been widely used in general circulation models: for example, it is currently used by the UCLA/GLA model and it provides the climatological values for deep soil moisture in the present ECMWF (European Centre for Medium Range Weather Forecasts) operational model (Brankovic and Van Maanen 1985). But the methods and assumptions used to derive this soil moisture climatology were never fully documented and discussed.

Land surface evapotranspiration is an important process in the weather and climate system of the Earth, and soil moisture, which partly determines the evapotranspiration, is an important variable of the system. By its influence on the vegetation structure, it also controls the solar radiation flux at the surface (the albedo effect) and the momentum flux at the surface (the roughness effect).

Eleven sensitivity studies reviewed by Mintz (1984) have demonstrated that the specification of albedo, roughness and, most importantly, the soil moisture have strong impacts in model-simulated climates. When soil moisture availability or surface albedo is changed regionally (or globally), changes in the precipitation, the temperature and the motion field of the atmosphere take place over the corresponding region (or over the globe), which are clearly above the level of the natural variability of the model simulated climates.

In spite of this, general circulation modellers have previously made only two attempts to determine the climatological soil moisture from observations. The first attempt was by Stone et al. (1977). They parameterized the ratio of actual to potential evapotranspiration β as a function of the surface air relative humidity RH, so that $\beta = 2(RH-15)/85$, $0 \le \beta \le 1$. The July value of β was equal or close to 1 over most of the land surface of the globe and produced the "excessive evapotranspiration" cases in the albedo sensitivity study by Charney et al. (1977). The other attempt was by Miyakoda et al. (1979) who took the observed normal precipitation from February to July, and somewhat arbitrarily relabeled the isolines of that antecedent precipitation as lines of equal β for the month of July. Because the antecedent evapotranspiration was not taken into account, they obtained a very small β value in the forest and tundra regions of northern Canada and Siberia, where, in fact, the soil is wet and evapotranspiration in July is considerable.

In the present study, the normal monthly available soil moisture and evapotranspiration are derived from the antecedent observed precipitation and an antecedent potential evapotranspiration. Although there are many approximations and assumptions in the formulation of our governing equations, they use as input data long series of observed precipitation and surface air tempera-

* Yale Mintz died on 27 April 1991. This work was carried out jointly over a number of years preceding his death

Offprint requests to: YV Serafini

ture which are among the easiest quantities to measure. Records of them are available over the continents going back many years. Our approach may be thought of as a compromise between the accuracy of the parameterization and that of the input data. In the next section we describe the successive developments of these water budget methods recently. The third section is devoted to the description of the model parameterizations, and the main results are shown and discussed in the penultimate section.

Existing water budget calculations

It was one of Thornthwaite's goals to produce a world atlas of the normal monthly potential evapotranspiration, actual evapotranspiration, and soil moisture; and towards that end he and his associate, J. R. Mather, collected the records of observed montly precipitation and surface air temperature from a large number of stations over the globe. By 1962, they had assembled the records from about 14800 stations. These were unevenly distributed over the globe and the length of the records varied from many decades to only one or two years. Tables of the monthly observed precipitation, calculated potential evapotranspiration, calculated evapotranspiration, and end-of-the-month soil moisture were published for 8565 of those stations (Mather 1962–1965); but the intended World Atlas was never constructed.

van Hylckama (1956) used the calculated root zone soil moisture from the Thornthwaite/Mather data set, together with a simple calculation of the amount of precipitation retained as snowcover, and an estimate of what was temporarily retained as groundwater beneath the plant root zone, to produce, with a horizontal resolution of 10° latitude by 10° longitude, the global fields of monthly total water mass stored on the continents.

Baumgartner and Reichel (1975), in pages 20–25 and plates, 5, 7, 10–14 and 17–20, used the calculated annual evapotranspiration at the 8565 stations in the Thornthwaite/Mather data set to produce a global map of annual evapotranspiration. Then they adjusted that field to make the area-averaged evapotranspiration, over each of the principal river catchment basins of the Earth, agree with the difference between the measured annual precipitation over the catchment and the measured annual river flow from the catchment. Except in the high latitudes of the Northern Hemisphere, those adjustments were relatively small.

A global map of the annual potential evapotranspiration was produced from station values in the Thornthwaite/Mather data set by Strahler and Strahler (1978, Fig. 10, 11). Strahler and Strahler (1978, pp 155–166) also formulated a climate classification scheme based on soil moisture and evapotranspiration. They used the Thornthwaite/Mather station values of monthly and annual mean soil moisture, evapotranspiration and potential evapotranspiration to construct a climate map of the world (Strahler and Strahler 1978, Plate D.2).

The same conceptual relationship between rainfall, potential evapotranspiration, actual evapotranspiration and soil moisture as those of Thornthwaite were used independently by M. Budyko and his associates to derive normal monthly potential and actual evapotranspiration at about 1500 stations over the globe. They have produced global maps of normal monthly potential and actual land surface evaportanspiration based on those station values (Zubenok 1965; Budyko 1963). Budyko and Zubenok, however, used an estimated net surface radiation flux to obtain the monthly potential evapotranspiration at each station. At each station location, their calculation produced not only the monthly evapotranspiration but also the soil moisture amount; but Budyko apparently published neither the station values nor maps of the calculated soil moisture.

Recently Willmott et al. (1985) produced a monthly climatology of soil moisture content. Their governing equations are very similar to ours, although they differ in some points: a treatment of the interception of rain by the vegetation is taken into account in our case, the effect of the snow cover is parameterized in their case. Also, an important difference between their study and ours arises from the different input data: Willmott et al. (1985) estimated the water budget cycle at each of the 13332 stations for which they have data, whereas we have used long-term monthly mean climatologies of the observed precipitation from Jaeger (1976) and surface air-temperature from the NCAR data archive (Spangler and Jenne 1984).

Governing equations and coefficients

Here we introduce the main notations and equations. The various assumptions and parameterizations implied by this approach are discussed in the following subsections.

Prognostic equation for the available soil moisture W

The soil moisture available for humidification of the atmosphere, which is the quantity called soil moisture by climatologists, is derived from a water budget equation, where its source is precipitation and its sinks are the evaporation terms from the ground, from the plant transpiration, or from the rain water intercepted by the leaves.

We take the change of available soil moisture over a day as:

$$\Delta W = (P - E_I) - (E_T + E_S), \quad O \leq W \leq W^* \qquad (1)$$

where:

W: available soil moisture (the amount of water in the root zone of the soil in excess of that at the vegetation wilting stage)
W^*: maximum available soil moisture (the difference between the field capacity of the soil and the amount of water in the soil at the vegetation wilting stage)
P: daily precipitation

E_I: daily interception-loss (the water that evaporates from the wet surface of the vegetation and soil during and immediately following precipitation)
E_T: daily transpiration (the water transferred from the root zone of the soil to the atmosphere through the root-stem-leaf system of the vegetation)
E_S: daily soil evaporation (the water that is directly transferred from the soil to the atmosphere by upward hydraulic diffusion through the pores of the soil)

In this study, the daily precipitation P is always treated as rainfall and $(P-E_I)<O$ is the daily infiltration of water into the soil. $(E_T+E_S+E_I)=E$ is the daily evapotranspiration. When $W=W^*$, $(P-E_I)>O$ is the daily surplus and contribution to the annual runoff.

Diagnostic equations for the interception-loss E_I and the transporation plus soil evaporation (E_T+E_S)

Given the precipitation P, the potential evapotranspiration E^*, and the soil moisture-dependent coefficient of transpiration plus soil evaporation β, the following equations are used to obtain E_I and (E_T+E_S):

$$\text{when } P=0 \begin{cases} E_I=0 \\ E_T+E_S=E^*\beta \end{cases} \tag{2a}$$

$$\text{when } P\geq E^* \begin{cases} E_I=E^* \\ E_T+E_S=0 \end{cases} \tag{2b}$$

$$\text{when } O<P<E^* \begin{cases} E_I=P \\ E_T+E_S=(E^*-P)\beta \end{cases} \tag{2c}$$

Here E^* is the daily potential evapotranspiration, or the amount of water vapor transferred to the air under the given atmospheric conditions, when the available moisture in the root zone of the soil and/or the water on the surface of the leaves and soil is not a limiting factor. This definition of potential evapotranspiration is subject to some uncertainties, since no measurement of the potential evapotranspiration can be made under strictly unchanged atmospheric conditions. By "given atmospheric conditions" we will mainly consider large-scale atmospheric conditions. How E^* is estimated from the mean daily surface air temperature and duration of daylight is considered in the next section. β is the coefficient that determines the ratio of (E_T+E_S) to (E^*-P). Later the dependence of β on (W/W^*), where (W/W^*) is the soil wetness, is described.

As indicated by Eq. (2a, b, c) on days when $P>E^*$ the surface of the vegetation and soil is assumed to be wet. On those days there is interception-loss at the potential evapotranspiration rate and there is no removal of moisture from the soil by transpiration or hydraulic diffusion. On days when $P<E^*$ all of the precipitation, of any, is removed as interception-loss and transpiration plus hydraulic diffusion removes moisture from the soil by the amount $(E_T+E_S)=(E^*-P)\beta$.

Since our input are monthly mean climatologies averaged over large grid areas, there is some inherent difficulty in trying to parameterize the various components of the total evapotranspiration. Our methods imply a continuous repartition of precipitation over the various days of the month. Where precipitation is time-variable or spatially inhomogeneous, the interception-loss will be overestimated. In regions where the ratio of actual to potential evapotranspiration β is equal to or not much smaller than 1, there will be about the same compensating underestimate of the transpiration plus soil evaporation (E_T+E_S) and, therefore, the total daily evapotranspiration $E=(E_T+E_T+E_S)$ as well as the surplus daily contribution to the annual runoff will not be significantly affected. But where β is much smaller than 1, the assumed uniform distribution of the precipitation will produce not only an excessive interception-loss but also an excessive total evapotranspiration $(E_I+E_T+E_S)$, and, consequently, an underestimation of the soil moisture W. It may be also thought that treating all precipitation as rainfall and none as snowfall will produce a significant error. But that, by itself, is not the problem, as we will see that in our case when $T_A\leq 0$, $E_I=0$ and $(E_T+E_S)=0$, P is then equal to the infiltration. This is the daily increase of soil moisture as long as $W<W^*$. When $W=W^*$, P is the daily surplus and contribution to the annual runoff. Now, if (as was done by van Hylckama 1956 and by Willmott et al. 1985) we were to treat precipitation as snowfall when $T_A\leq 0$ and accumulate it as a snowcover which melts when T_A first exceeds zero, then the infiltration of the water into the soil, and any contribution to the annual runoff, would take place at the time of melting. But the daily E_I and daily (E_T+E_S) throughout the year, and also the annual surplus and runoff, would be exactly the same as when all the precipitation is treated as rainfall. That this is in fact the case was shown by Willmott et al. (1985, p. 594 and Fig. 2). However, as discussed in the fourth section, the reduction of the field capacity by freezing of the ground has an important effect, which we neglect in the present study.

Thornthwaite's empirically derived formula for the potential evapotranspiration E^* (T_A, h)

Generalities. When land surface evapotranspiration takes place at the potential rate, the equation of energy conservation at the land surface, integrated over a day, is:

$$R_n-G-LE^*-H^*=0, \tag{3}$$

or, with a rearrangement of the terms,

$$LE^*=(R_n-G)[1+B_o^*]^-1 \tag{4}$$

where:

$$B_o^*=\frac{H^*}{LE^*}$$

R_n: net daily downward radiation flux at the surface,
G: net daily sensible heat storage in the vegetation and in the soil,
E^*: daily potential evapotranspiration,
H^*: daily upward flux of sensible heat at the surface, under potential evapotranspiration conditions

L: coefficient of latent heat, and
B_o^* is the Bowen ratio under potential evapotranspiration conditions.

Priestley and Taylor (1972) showed that if we assume the same eddy diffusion coefficients for sensible heat and water vapor, and consider only areas which are large enough to neglect horizontal advection effects, we have:

$$B_o^* = \left(\frac{\Delta+\gamma}{\alpha\Delta}\right) - 1 \tag{5}$$

and substituting for B_o^* in Eq. (4), we obtain:

$$E^* = \alpha\left(\frac{\Delta}{\Delta+\gamma}\right)(R_n - G)L^{-1} \tag{6}$$

where:

Δ: $(\partial q^*/\partial T)$ is the rate of change of water vapor saturation mixing ratio with temperature, taken at the temperature of the surface air,
γ: C_p/L
C_p: specific heat of air at constant pressure
α: unknown scaling coefficient

Another commonly used expression for E^* was derived by Penman (1948), who combined the equation for energy conservation at the Earth's surface with the aerodynamic (bulk mass transfer) equation for water vapor, and applied this to a surface that is sufficiently moist for the air in contact with the surface to be saturated. He then found:

$$E^* = \frac{\Delta}{\Delta+\gamma}\,\frac{R_n - G}{L} + f_e(u_r)(e_r^* - e_r), \tag{7}$$

where R_n is the net (all wavelength) downward radiation flux at the surface, G is the flux of sensible heat from the surface into the underlying vegetation and soil, $f_e(u_r)$ is an empirically (or theoretically) determined function of some short period averaged wind speed at a reference level in the air above the surface (this function depends on the surface roughness and thermal stability of the air), e_r is the short period averaged vapor pressure of the air at the reference level, $e_r^* = e^*(T_r)$ is the saturation vapor pressure at the reference level air temperature T_r, $\Delta = (de^*/dT)$ is the rate of change of the saturation water vapor pressure with temperature at the temperature T_r, $\gamma = C_p p/(\mathrm{L}\ 0.622)$ is the psychrometric constant, and L is the latent heat of vaporization.

Thornthwaite's approach

Thornthwaite knew in 1948 that the potential evapotranspiration depends mainly on the net radiational heating of the land surface and, to a lesser extent, on the surface air wind speed, temperature and relative humidity. He believed, however, that it would be a long time before either measurements or sufficiently accurate calculations of the net radiational heating of the surface would be available from more than just a few experimental sites and, therefore, that the surface radiation information would not be available for a reliable global climatology of the potential evapotranspiration. Indeed, this is still the case.

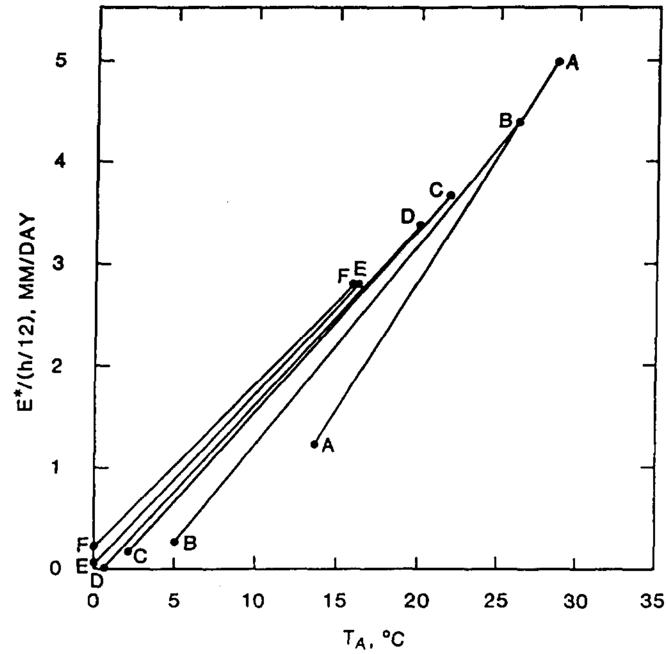

Fig. 1. Measured daily potential evapotranspiration normalized to a 12-hour day, as a function of the daily mean surface air temperature. *A*: Kissmee, Florida; *B*: Mesilla Valley, New Mexico; *C*: Coshocton, Ohio; *D*: North Platte, Nebraska; *E*: San Luis Valley, Colorado; *F*: New Fork Valley, Wyoming. (Redrawn from Thornthwaite 1948, Fig. 2)

As an alternative to the unavailable net radiation flux at the surface, Thornwaite (1948) decided to use the available surface air temperature as a substitute, which he would empirically relate to the potential evapotranspiration. He compared T_A, the measured daily mean surface air temperature, with $E^*/(\mathrm{h}/12)$, the measured daily potential evapotranspiration normalized to a 12 hour length of day at a number of test sites in the United States. He used all available data, from lysimeter data to water budget calculations over irrigated valleys. He found, as shown in Fig. 1, that at each site there was a linear increase of $E^*/(\mathrm{h}/12)$ with increasing T_A; that the rate of change $\partial(E^*/(\mathrm{h}/12))/\partial T_A$ increased with the average annual temperature of the test site; and that the curves converged near $T_A = 26.5°\mathrm{C}$, where $E^*/(\mathrm{h}/12) = 4.5$ mm/day.

From these empirical relationships, Thornthwaite (1948) obtained the regression of E^* upon T_A, h:

$$E^* \begin{cases} = 0 \\ = 0.444\, h(10\, T_A/I)^a \\ = -13.862 + 1.0747\, T_A - 0.01442\, T_A^2 \end{cases} \tag{8a}$$

when $T_A < 0°\mathrm{C}$
when $0 \le T_A < 26.5°\mathrm{C}$
when $26.5 < T_A$

$$I = \sum_1^{12} i, \quad i = (T_M/5)^{1.514}, \; i_{\min} = 0 \tag{8b}$$

$$a = (6.75 \times 10^{-7} I^3) - (7.71 \times 10^{-5} I^2) + (1.792 \times 10^{-2} I) + 0.49239 \quad (8c)$$

where

E^* = daily potential evapotranspiration, mm/day.
h = length of the day, hours.
T_A = daily mean surface air temperature, °C.
T_M = normal monthly mean of T_A, °C.
I = index of the annual daily mean surface air temperature.

Figure 2a shows $E^*/(h/12)$, the daily potential evapotranspiration (mm/day) normalized to a 12 hour day, as a function of the daily mean surface air temperature T_A, and the annual daily mean surface air temperature index I. The global annual temperature index is given in Figure 2b. Figure 3a, b show the resulting global maps of the potential evapotranspiration for the months of January and July. These results may be compared to those of Zubenok (1965). The main discrepancies appear over arid or semi-arid areas where Zubenok's values are higher. This will be discussed further in the next section. There is, however, some difficulty in estimating the potential evapotranspiration in arid regions, since the available large-scale parameters are for real conditions, not potential ones; in this case the empirical formulae of Thornthwaite may no longer be valid.

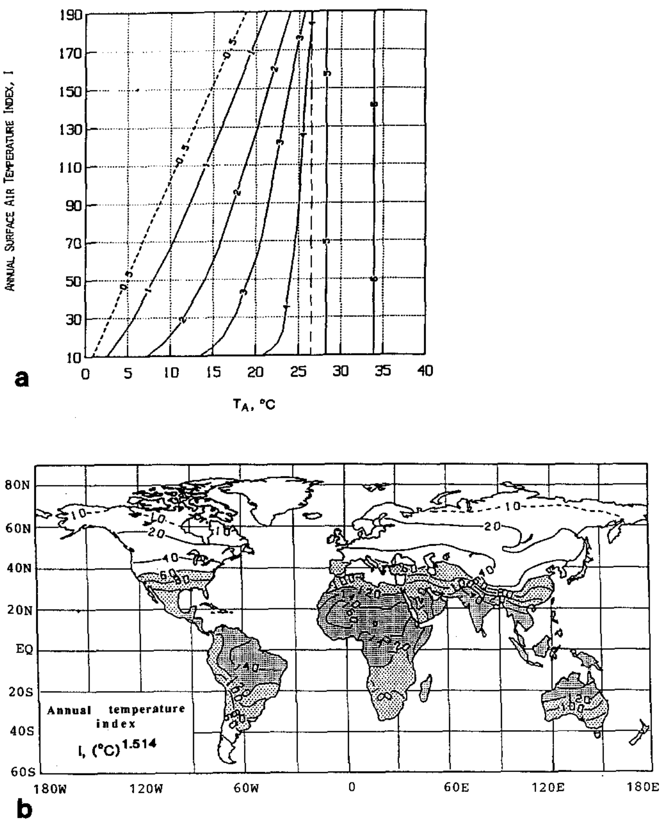

Fig. 2a. Daily potential evapotranspiration normalized to a 12-hour day, as a function of the daily mean surface air temperature T_A and the annual surface air temperature index I. (From the Thornthwaite 1948 regression equation); **b.** Annual surface air temperature index I

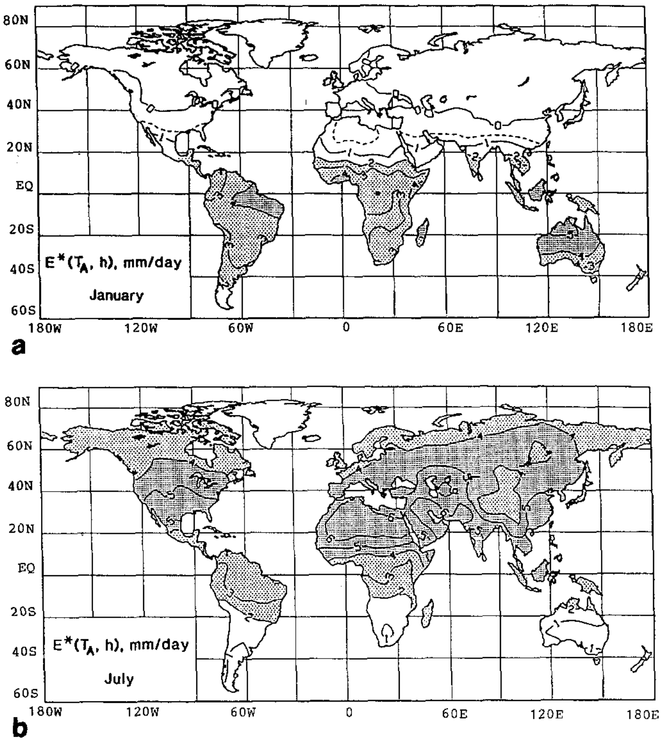

Fig. 3. a Global map of the potential evapotranspiration (mm/day) for the month of January as obtained from the Thornthwaite method; **b** Global map of the potential evapotranspiration (mm/day) for the month of July as obtained from the Thornthwaite method

Making E^* a function of T_A, h, and I, as Thornthwaite and Hare (1965) said, is "... only an approximation, to be replaced whenever a fully rational predictor of E^* becomes available. Its success depends on the fact that the mean air temperature does, to a considerable extent, serve as a parameter of the net radiation ..."

Justification of Thornthwaite approach

A rationale for Thornthwaite's method can be derived from Eq. (4). Δ increases with increasing temperature and, therefore, B_o^* decreases and $[1+B_o^*]^{-1}$ increases with increasing T_A.

In Fig. 4a (from Brutsaert 1982, Fig. 10.3) the plotted points are measured daily values of B_o^* as a function of T_A from open water surfaces and from land surfaces covered with low (groundcover) vegetation that is actively growing under potential (moist soil) conditions. The two curves in Fig. 4 show B_o^* as a function of T_A from Eq. (5) when $\alpha = 1.26$ and when $\alpha = 1.28$. As stated by Brutsaert (1982 pp 220), "It is remarkable that so many land surfaces covered with fairly short vegetation, such as grass, which is not actually wet but which has ample water available, yield about the same value of 1.26 to 1.28 as open water surfaces."

Figure 4b shows $[1+B_o^*]^{-1}$ as a function of T_A for $\alpha = 1.27$. When $T_A = 0$° C, $[1+B_o^*]^{-1} = 0.55$ and by Eq. (4), $LE^* = 0.55\ (R_n - G)$. When $T_A = 30$° C, $1+B_o^*]^{-1}$

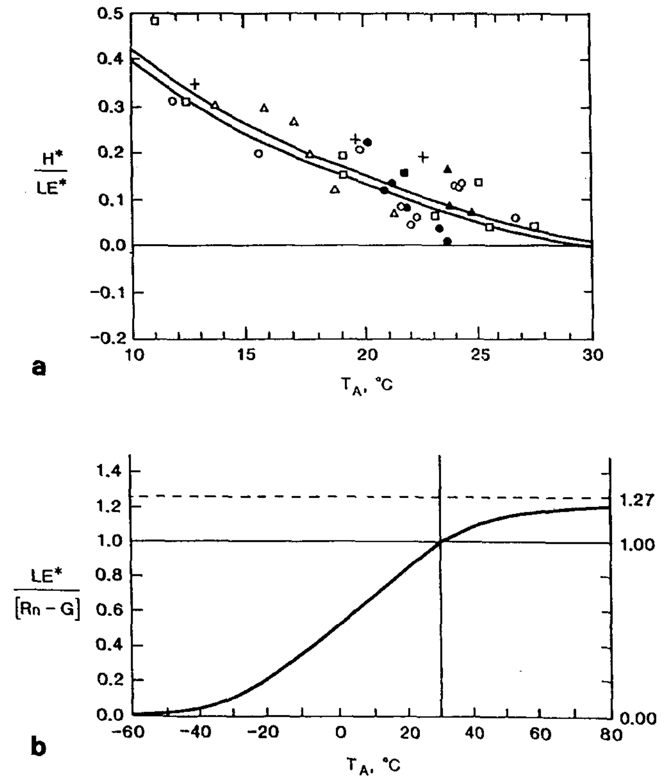

Fig. 4. a Variation of the Bowen ratio with surface air temperature at freely evaporating surfaces. The data points (for daily values) were collected by Davies and Allen (1973) from various field studies. The *upper curve* represents $\alpha = 1.26$ and the *lower* $\alpha = 1.28$ in the theoretical relationship derived by Priestley and Taylor (1972) (from Brutsaert 1982); b Variation of $(1 - B_o^*)^{-1}$ with air temperature when $\alpha = 1.27$

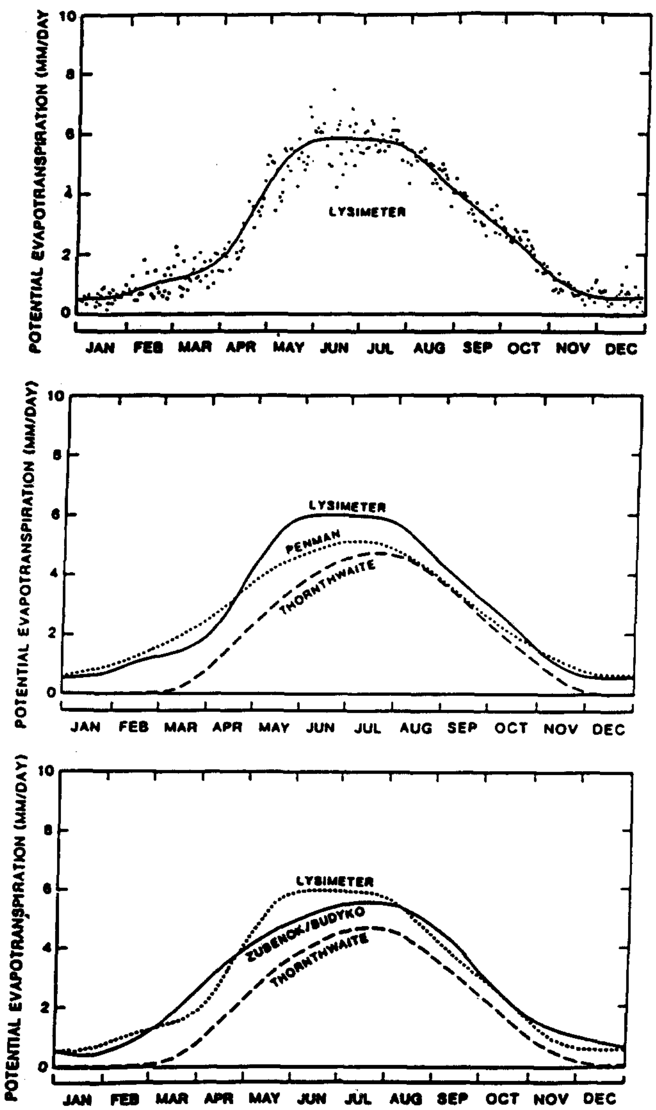

Fig. 5. Potential evapotranspiration at Coshocton, Ohio. *Top:* 15 year averages of daily potential evapotranspiration E^* as measured by deep rooted grass lysimeters; *Center*: E^* as measured by the lysimeters and as calculated with the Penman and Thornthwaite equations; *Bottom*: E^* as measured by the lysimeters, as calculated with the Thornthwaite equation, and as read from the maps of normal monthly potential evapotranspiration calculated by Zubenok (1965) with the Budyko equation

$=1$ and $LE^* = (R_n - G)$. When T_A exceeds 30° C, $B_o^* < 0$, $[1 + B_o^*]^{-1} > 1$ and $LE^* > (R_n - G)$. The upper limit is $LE^* = 1.27\ (R_n - G)$.

In the case of tall vegetation (trees), H^* and LE^* are very difficult to measure. But such field measurements as have been made show that the corresponding α is somewhat smaller with trees than with groundcover. McNaughton and Black (1973) found that $\alpha = 1.05$ for a young, 8 m-high Douglas fir forest, when the roots of the trees were well supplied with water but the leaves were not wet.

Figure 5 compares the potential evapotranspiration as calculated with the Thornthwaite regression equation; as calculated with the radiation-aerodynamic equation of Penman (1948); and as measured with lysimeters (from McGuiness and Bordne 1972, Tables 19, 29, 33). These results are mainly illustrative since the sign of the difference between the various estimates may vary from one lysimeter to the other (as stated by Mc Guiness and Bordne 1972), and Thornthwaite's method in many cases overestimates the potential evapotranspiration.

The top panel in Fig. 5 (McGuiness and Bordne 1972, Fig. 1) shows the evapotranspiration measured with deep-rooted grass-covered weighing lysimeters at Coshocton, Ohio (40° N, 82° W), over a 15-year period. (The years 1948–1965, minus the years 1956, 1957 and 1964 when the grass cover was being renewed and minus the 15 to 30 days following each hay cutting; and with an empirical correction made to the measured evapotranspiration whenever the measured moisture in the uppermost 100 cm of the lysimeter showed limiting soil moisture.) The plotted points show the 15-year averages of the measurements made on each calendar day of the year (which, in spite of the 15-year averaging, still show large differences between adjacent days); and the solid curve shows the five-term harmonic of best fit to the daily averages. This is also the solid curve in the center panel of Fig. 5. Mustonen and McGuiness (1968) have shown that the lysimeter evapotranspiration values obtained were too high, and in our comparison we shall mainly retain the seasonal shape of the curve, which, on the contrary, seems correct. The dotted curve in the center panel shows the potential evapotranspiration as calculated with the Penman equation. It is important to note that the dominant term in the Penman equation is the radiation term, and that only the incident solar flux was measured; monthly albedo from a meadow near Vienna (Austria) was used, and the longwave (infrared) component was taken from an empirical formula of Penman (1948). In the bottom panel of Fig. 5 is the normal monthly potential evapotranspiration at the Coshocton location (40° N, 82° W), as read from the global maps produced by Zubenok (1965), who used the Budyko (1956) equivalent of the Penman equation. For both the central and bottom panels the Thornthwaite estimate is shown as dashed lines, as obtained by McGuiness and Bordne (1972).

We see that the Penman calculation, the Zubenok estimate and the lysimeter measurements are closer in phase to the declination of the sun than is the Thornthwaite calculation. This phase error was noted by Thornthwaite and Hare (1965) and attributed to the fact that in the extratropics the mean surface air temperature typically lags behind the sun declination by about a month. We compared the Thornthwaite calculation with the Budyko calculation in several regions over the Earth, and concluded that where the soil is moist the two calculations produce roughly the same results in the summer season in the extratropics, and throughout the year in the tropics; and it is only in the winter extratropics (when both R_n and T_A are small) that the Thornthwaite calculation is larger than the Budyko calculation. But in regions of dry soil and desert regions, the potential evapotranspiration calculated with the Thornthwaite method is always smaller than that calculated with the Budyko method.

The Thornthwaite calculation of potential evapotranspiration is used operationally all over the world and has been the subject of a very large number of comparisons with measurements. The US Weather Bureau (NOAA) and the US Department of Agriculture use the Thornthwaite (1948) regression equation for $E^*(T_A, h)$ to produce their weekly and monthly Palmer Drought Severity Index (PDSI) and Crop Moisture Index (CMI) maps for the United States (see Palmer 1965, 1968; Mather 1974 and NOAA/USDA, *Weekly Weather and Crop Bulletin*). It is also used by the Canadian Climate Centre, Downsview, Ontario, to produce the weekly maps of available soil moisture in Canada (see Louie and Pugsley 1981).

Dependence of the coefficient of transpiration plus soil evaporation β on the soil wetness W/W^*

In his initial soil moisture budget calculations, Thornthwaite (1948) let:

$$\beta \begin{cases} =1 & \text{when } (W/W^*)>0 \\ =0, & \text{when } (W/W^*)=0 \end{cases}$$

which means that the transpiration plus soil evaporation equals the potential evapotranspiration (or equals the excess of the potential evapotranspiration over the precipitation) as long as there is any available moisture left in the soil.

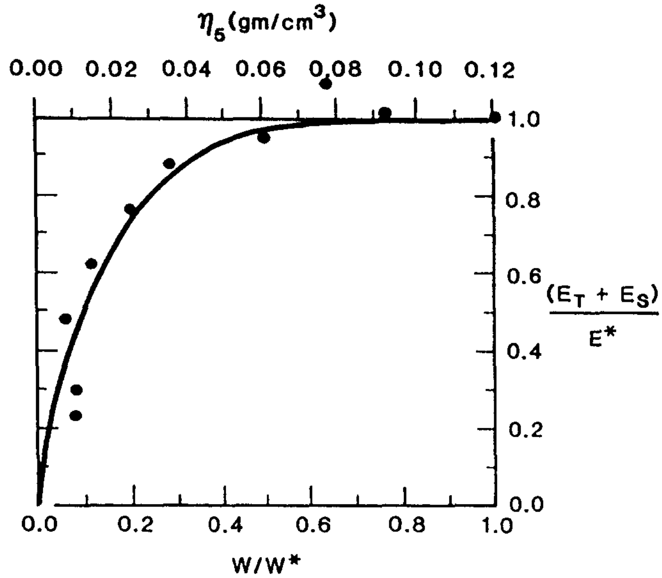

Fig. 6. Ratio of the measured transpiration plus soil evaporation to the measured potential evapotranspiration, $(E_T+E_S)/E^*$, on days without precipitation, as a function of the measured near-surface soil moisture η_5 and the estimated root zone soil wetness W/W^* (adapted from Nappo 1975)

Later, Thornthwaite (1954, Fig. 1) let $\beta = W/W^*$. This was the relationship obtained by Halstead (1954) from the measured soil moisture, the measured net radiation and the calculated evapotranspiration during five observing periods in the O'Neil, Nebraska, Great Plains Field Experiment (Lettau and Davidson 1957). It was this linear relationship between β and W/W^* that was used by Thornthwaite and Mather to produce the large data set of station evapotranspiration and soil moisture (Mather 1962–65). For his calculations of the evapotranspiration and soil moisture, Budyko (1963) used a dependance of β on W/W^* which varied geographically and with the season of the year.

We will use an adaptation of the relationship between $(E_T+E_S)/E^*$ and soil moisture (on days without precipitation) as derived by Nappo (1975) from field measurements made by Davies and Allen (1973). In their field study, which was made during a summer in southern Ontario (42° N), Davies and Allen used the energy balance/Bowen ratio method to obtain the daily values of (E_T+E_S) from two adjacent (122 m × 67 m) fields, each of which had a continuous cover of perennial rye grass growing in a sandy loam soil, and where one of the fields was irrigated. Nappo (1975) took the ratio of (E_T+E_S) from the non-irrigated field to that from the irrigated field, both taking place under the same atmospheric conditions, to be $(E_T+E_S)/E^*$, and plotted this ratio against η_5, the measure volumetric soil moisture in the upper 5 cm of the non-irrigated field. His data points and exponential curve of best fit are shown in Fig. 6.

We have assumed that the continuous grass cover, by shading the soil from sun, makes the soil evaporation

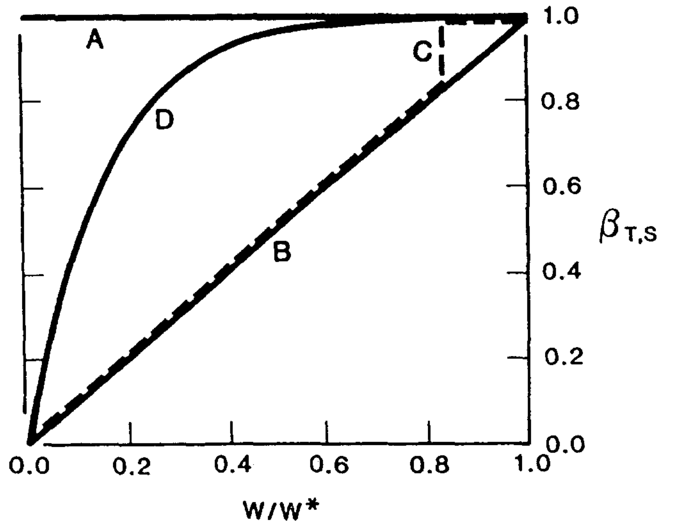

Fig. 7. $\beta=(E_T+E_S)/(E^*-P)$ as a function of the soil wetness W/W^*. A: Thornthwaite (1948); B: Thornthwaite and Mather (1955); C: Present study; D: Palmer (1965)

very small and, consequently, that the soil moisture is approximately constant with depth over the root zone. This gives as the curve of best fit

$$\beta=1-\exp^{-6.8(W/W^*)}. \tag{9}$$

As shown in Fig. 7, this dependence of β on the soil wetness W/W^* is intermediate between the two relationships used by Thornthwaite, but is closer to his original choice.

There is a large literature on the coefficient of transpiration and soil evaporation and, as shown in the reviews by Rutter (1975 pp. 147-150) and by Ward (1975 pp. 104-108), β depends on more than just the soil wetness. But because the soil wetness is the main determinant and closes our system of equations, we shall use this relationship for the present calculations. For a more realistic treatment it would probably be better not to construct a more complex function for β, but instead to devise a numerical model of the Earth's vegetation cover which is more directly based on biophysical principles, such as that proposed by Sellers et al. (1986) and Mintz and Sellers (1986).

Soil moisture storage capacity W^*

There are two ways to obtain the moisture storage capacity of the root zone of the soil:
1. from the soil properties and effective root depth,
2. from the time integral of measured evapotranspiration minus precipitation.

W^* from the soil properties and the effective root depth. Table 1 shows, for different types of soil arranged in the order of decreasing soil particle sizes, the volumetric soil moisture field capacity w_{FC}; the volumetric soil moisture wilting point w_{WP}; and the volumetric available soil moisture storage capacity $w^*=(w_{FC}-w_{WP})$; all are in units of gm/cm^3 (data from Smith and Ruhe 1955). We see that although both w_{FC} and w_{WP} vary by more than a factor of two, w^* has a much smaller variation. In fact, w^* is about 0.15 ± 0.03 gm/cm^3 for all the soils except fine sand.

Table 1. Water holding properties of soils

Soil type	w_{fc} gcm^{-3}	w_{wp} gcm^{-3}	$w^*=(w_{fc}-w_{wp})$ gcm^{-3}
Fine sand	0.125	0.033	0.092
Fine sandy loam	0.217	0.067	0.150
Loam	0.267	0.100	0.167
Silt loam	0.292	0.117	0.175
Clay loam	0.317	0.150	0.167
Clay	0.333	0.208	0.125

Average w^* for all soil types $=0.146$ gcm^{-3}

where w_{fc} is the volumetric field capacity, w_{wp} is the volumetric wilting point, $w^*=(w_{fc}-w_{wp})$ is the volumetric soil moisture storage capacity (from Smith and Ruhe 1955)

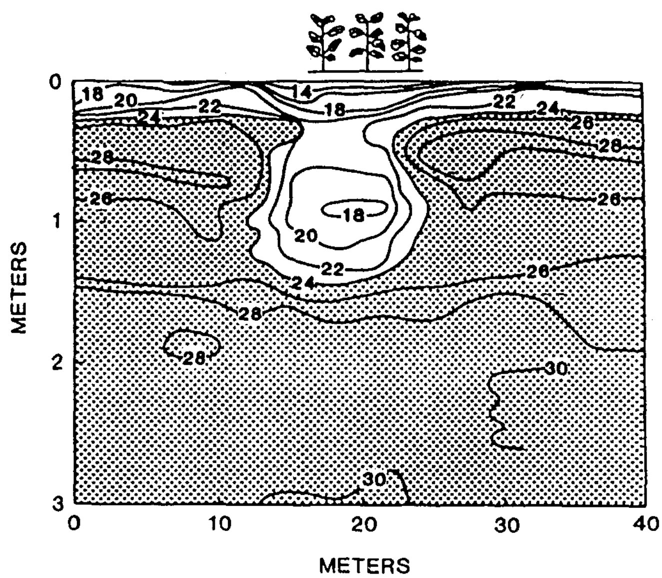

Fig. 8. Soil moisture (%) sampled across a line of oak trees in a fallow field (from Miller 1977, after Rode 1969)

Although the volumetric soil moisture storage capacity w^* has only a small variation, the naturally occurring root depths have large space and time variations.

Figure 8 is an instructive example of soil moisture sampled across a line of oak trees in a fallow field (from Miller 1977, Fig. IX,2, after Rode 1969). Away from the trees the soil moisture is depleted to a depth of about 20 cm, while under the trees the soil moisture is depleted to a depth of about 150 cm. Therefore, with $w^*=0.15$ gm/cm^3, $W^*=\int w^*\delta z$ will be about 30 mm in equivalent water depth in the fallow field away from the trees, and 225 mm under the trees. Miller (1977 pp 224) states: "Depletion of soil moisture by woody vegetation, which usually is deep rooted, reaches a large total over a year because the trees or shrubs experience fewer days of limited moisture supply than does herbacious vegetation.

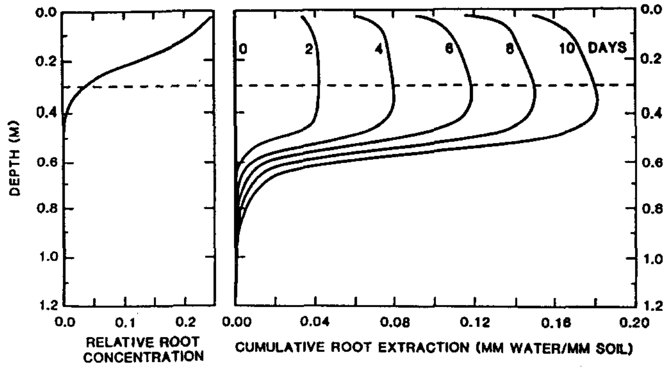

Fig. 9. Numerical simulation of the extraction of soil moisture by the roots of a field crop (from Hillel 1977). As shown by the *dashed line*, the water extraction occurs deeper than the root concentration profile would indicate

Green trees amid an expanse of baked, sundried grass are a familiar sight, representing continued availability of soil moisture at depths greater than grass roots can reach".

Roots extract soil moisture from a greater depth than one might at first assume from a vertical profile of the root length density. This can be seen in Fig. 9, which shows a numerical simulation of the extraction of soil moisture by the roots of a field crop (Hillel 1977, pp. 168–189). The simulation prescribed a constant daily transpiration E_T of 10 mm/day, with a sinusoidal diurnal variation; a soil evaporation E_S that was 0.02 times the transpiration; an initial volumetric soil moisture of 0.25 gm/cm^3 at all depths (the volumetric field capacity of loam soil); a total root length of 10000 m of roots per m^2 of field, with the vertial distribution shown on the left in Fig. 9; and state of stress on the plants, producing wilting when the crown potential falls to −30 bars.

The curves on the right in Fig. 9 shows the cumulative root extraction of soil moisture (the cumulative effect of E_T) as a function of depth, at intervals of 2 days from the initial state to the end of day 10. On the eleventh day wilting began. Only about 5% of the roots are below the depth of 30 cm, shown by the horizontal dashed line; but these few roots account for about half of the 100 mm of water extracted. With $w^* \simeq 0.15$ gm/m^3, the effective rooth depth is 100/0.15 mm, or 67 cm. This is twice the depth reached by 95% of the roots.

W^* from the time integral of measured evapotranspiration minus precipitation. If we integrate Eq. (1) from a time t_0 when $W = W^*$ until a time t_1 when $E = (E_I + E_T + E_S) = 0$, and do this over periods without runoff, we obtain:

$$W^* = \int_{t_0}^{t_1} (E - P)\,\delta t.$$

The starting time t_0 must be one preceding which there was sufficient rainfall (or irrigation) to be certain that W equals W^*; there must be a reliable measurement of the subsequent precipitation (or irrigation), and a reliable determination of the evapotranspiration $(E_I + E_T + E_S)$.

Priestley and Taylor (1972 Figs. 3, 4, 5) and Ritchie et al. (1972 Fig. 2) give examples of W^* obtained in this way for various field crops. Their values of W^* range from about 95 mm to 240 mm, all of these being about twice what one might expect from the apparent depth of the roots of those crops.

W^* has not been obtained in this way for forest vegetation, because there have been no forest measurements of evapotranspiration from field capacity to wilting stage. For the present study, we will use $W^* =$ constant $= 150$ mm, this being, perhaps, the average value for all types of vegetation. Initially, Thornthwaite (1948) used $W^* = 100$ mm everywhere, while later Thornthwaite and Mather (1955) used $W^* = 300$ mm everywhere. Louie and Pugsley (1981) produced their weekly soil moisture maps for Canada by letting W^* vary with location from 100 mm to 280 mm, depending not on the vegetation type but on the soil type.

Results

This section describes the calculation procedure and gives the main global fields obtained. Their signification and validity is discussed.

Calculation procedure

We calculate the soil moisture by writing Eq. (1) as

$$W_D = W_{D-1} + (P - E_I)_D - (E_T + E_S)_D, \quad 0 \leq W_D \leq W^* \quad (10)$$

where W_D is the soil moisture at the end of day D; W_{D-1} is the soil moisture at the end of the preceeding day; $(P - E_I)_D$ is the infiltration into the soil during day D; and $(E_T + E_S)_D$ is the transpiration plus soil evaporation during day D, as calculated with Eqs. (2a, b, c) and (8a, b, c), using P, T_A, h_D and W_{D-1}.

If, at the end of the day, the calculated W_D exceeds W^*, then W_D is set equal to W^* and the surplus is taken as that day's downward percolation through the base of the root zone of the soil and, therefore, that day's contribution to annual runoff.

The precipitation P_D and potential evapotranspiration E_D^* for each day of the month, are taken as equal to their monthly mean values. By Eq. (2), this also makes the infiltration $(P - E_I)_D$ constant over the month. However, by Eqs. (10) and (2), the soil moisture W_D and the transpiration plus soil evaporation $(E_T + E_S)_D$ change from day to day during the month.

The solution is obtained by letting W_{D-1} equal any arbitrary initial value, on some arbitrary day, and then carrying the calculation forward in one day time steps until the difference between W_D on the same calendar day of two successive years approaches zero. As noted earlier, this study uses as input monthly mean values of precipitation from Jaeger (1976) and surface air temperature from Spangler and Jenne (1984) on a 4°×5° grid.

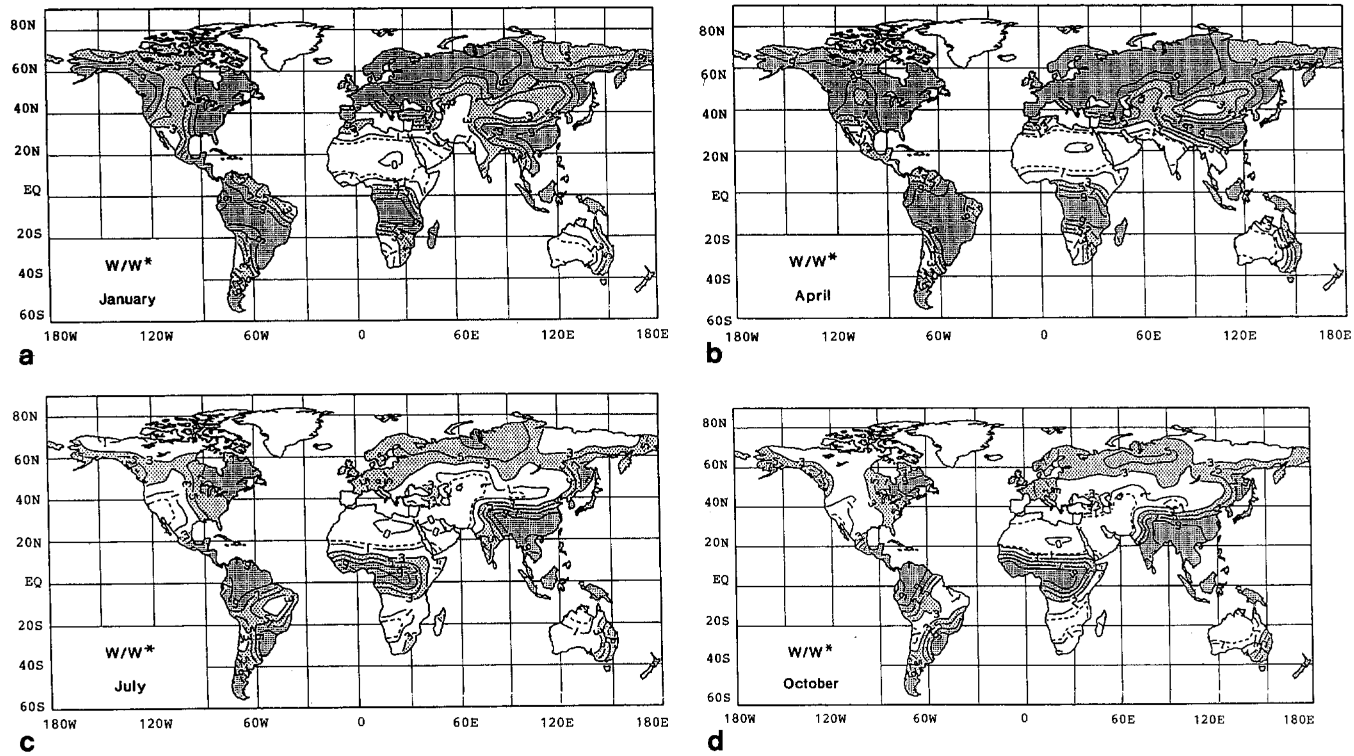

Fig. 10. a–d. Derived soil moisture distributions for the months of January, April, July and October, respectively. In tenths of the field capacity. **e–p** Color maps of the monthly distribution of the soil moisture over the annual cycle (courtesy of Lydia Dümenil, MPI, Hambourg. In fraction of field capacity

Description of the derived monthly fields

The derived monthly fields are available on request in digital form (magnetic tapes for example). They were already presented in Serafini (1986) and Mintz and Serafini (1989). The purpose of the present section is to show some of the main features of these distributions.

The soil moisture distributions for January, April, July and October are shown in Fig. 10a, b, c, d. Moreover color illustrations of the monthly means over the annual cycle are shwon in Fig. 10e–p. The corresponding distributions for the evapotranspiration are shown in Fig. 11a, b, c, d, and the mean annual run-off is shown in Fig. 12.

The soil moisture values show a strong seasonal cycle at mid- or higher latitudes. This is mainly due to a corresponding variation in the potential evapotranspiration: in winter it is too low to remove water efficiently from the soil and a large part of the precipitated water remains stored in the ground or is drained out. In summer the potential evaporation increases and produces a larger drying. The seasonal cycle for evapotranspiration is therefore almost inverse: the evapotranspiration rate is very low in winter, and is mainly driven by the precipitation rate in summer.

At low latitudes where the potential evapotranspiration is large, the seasonal cycle also closely follows the forcing by precipitation. It is interesting to note that, in spite of the disagreement of many features of our potential evapotranspiration distributions with those of Zubenok (1965), noted in the third section, our evapotranspiration distributions are in somewhat better agreement with those of Budyko (1963) which were derived using Zubenok's potential evapotranspiration. This is especially the case in arid regions, where the largest difference was found between the estimate of the potential evapotranspiration by the Zubenok and Thornthwaite methods, but where the corresponding actual evapotranspiration are in much closer agreement, although our estimates remain lower than those of Budyko. Conversely our evapotranspiration rates tend to be larger than Budyko's estimate in wet regions. It should be noted that, apart from the calculation of the potential evapotranspiration, the parameter β and the drainage were also specified differently in Budyko's work. These parameterizations varied according to the location and were apparently never fully published.

The total runoff distribution follows closely the distribution of the precipitation fields, but with values approximately two-thirds lower, due to the evaporation (Fig. 12). It is one of the few results that can be verified against real data, at least at the scale of a large river basin; this is done in a later section.

Discussion of the principal assumptions and approximations

A number of simplifying assumptions and approximations were made to obtain the closed calculation scheme for the soil moisture and evapotranspiration. An idea of how much these simplifications can affect the resulting

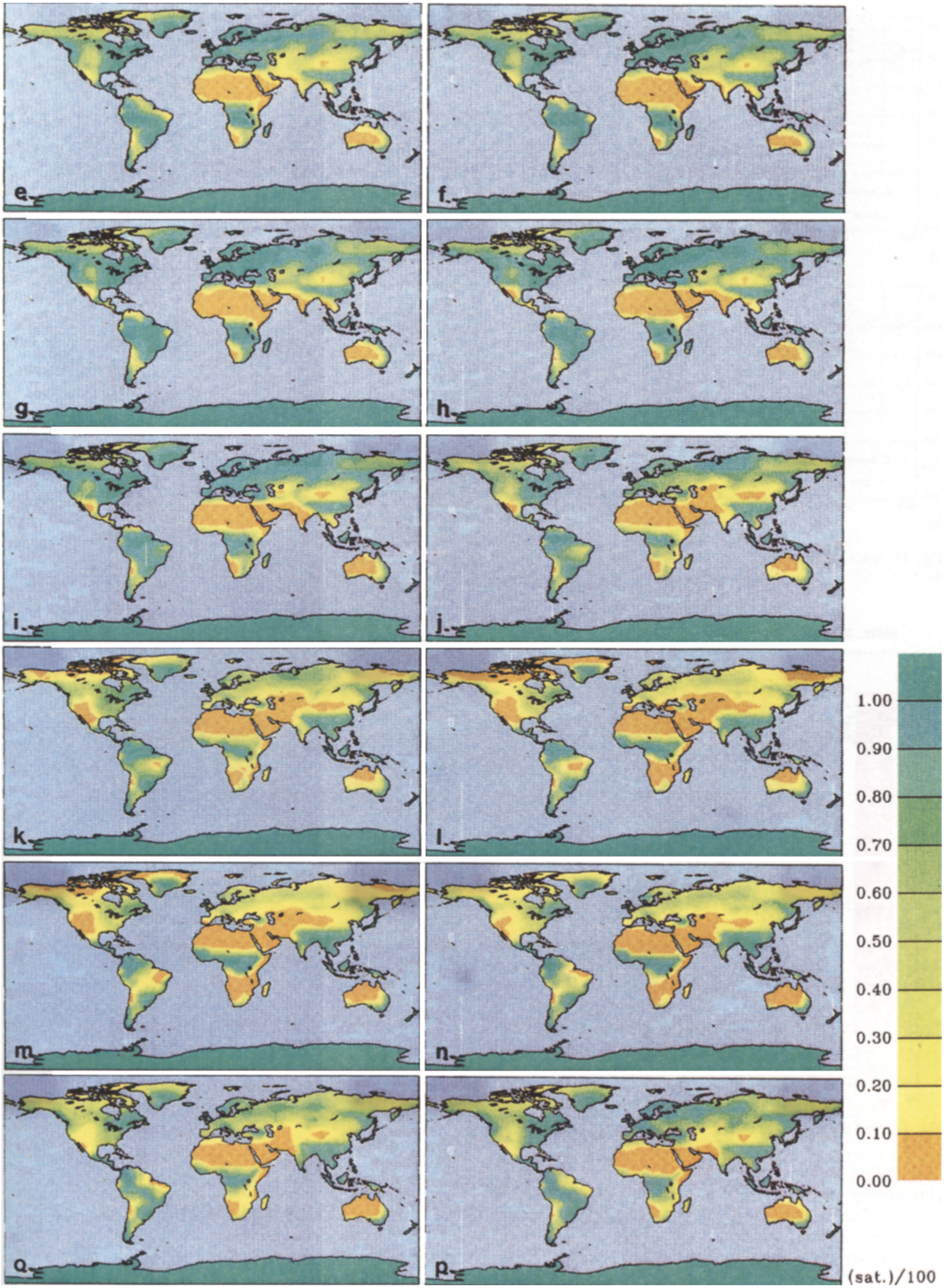
e
f
g
h
i
j
k
l
m
n
o
p
1.00
0.90
0.80
0.70
0.60
0.50
0.40
0.30
0.20
0.10
0.00
(sat.)/100

Fig. 10e–p

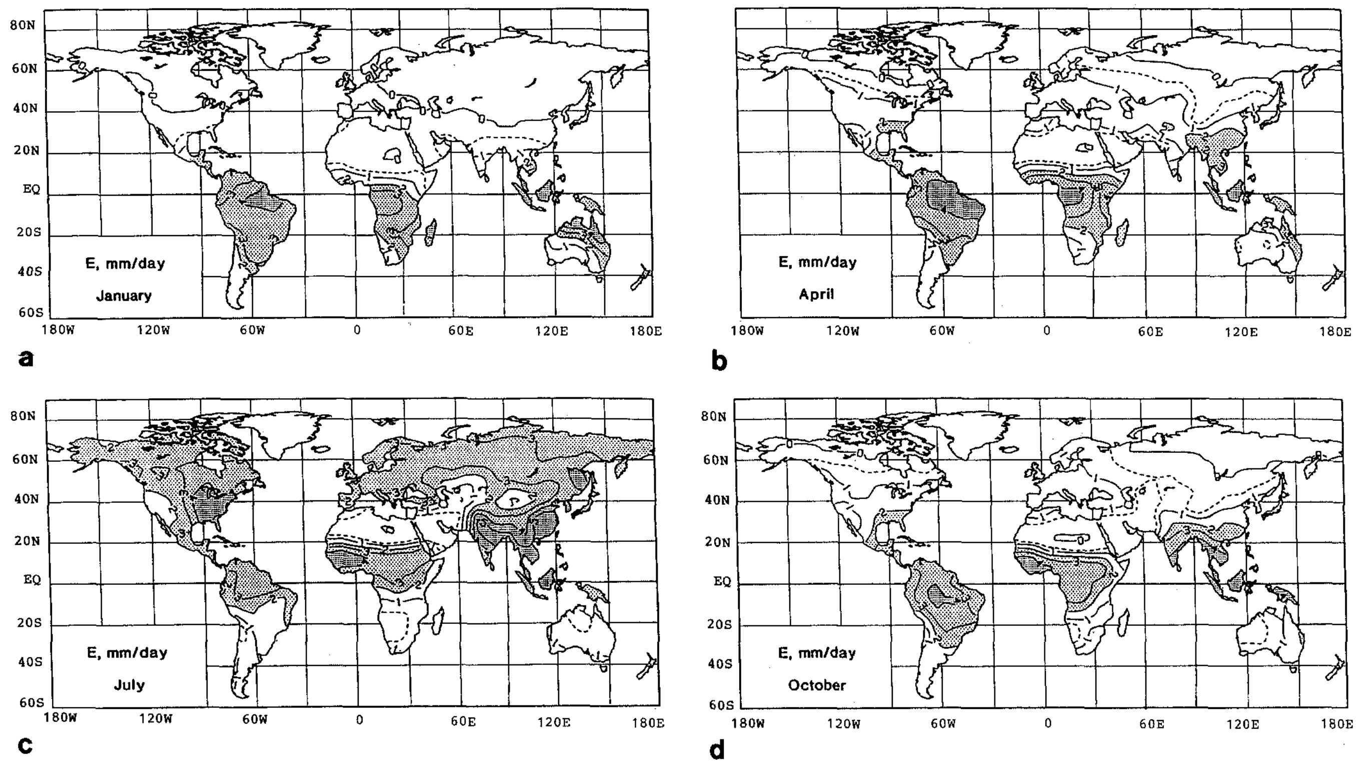

Fig. 11. a–d. Derived actual evatranspiration distributions for the months of January, April, July and October, respectively (in mm/day)

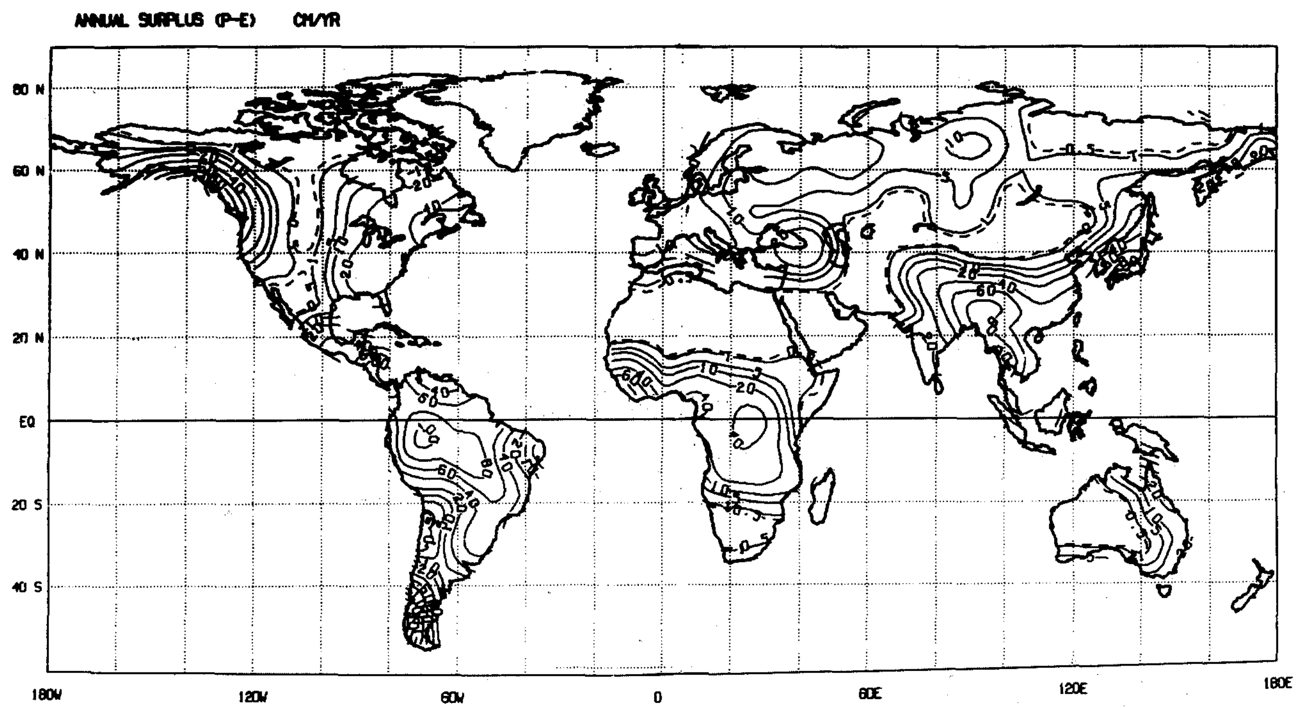

Fig. 12. Derived annual run-off distribution (in cm/year)

climatology can be seen from the results of Serafini and Sud (1987). In those sensitivity studies the forcing term (i.e., precipitation) was set to zero and a drying time of the soil was derived, starting from the climatology described in the present work. In all the regions where a short drying time is obtained, the evapotranspiration rate is primarily determined by the precipitation rate, and does not depend too much on the assumptions made in the model: but the soil water storage depends a lot on these assumptions. This is mainly the case at low latitudes or in the summer hemisphere at mid-latitudes. Reversely, when the drying time is large, the soil stores or drains out most of the precipitation, and the resulting water storage is little affected by the model assumptions concerning the evapotranspiration. But the rate of evapotranspiration, however low, is known with some imprecision.

The main sources of imprecision in our calculations are the following:
1. The empirical relationship between E^* and T_A and h was obtained from measurements made under potential (i.e., moist soil) conditions. But when we apply Eq. (8) to arid and semi-arid regions where the soil is dry, the surface air temperature will be higher than that with the same net radiational heating under potential conditions. Consequently, the calculated E^* in arid and semi-arid regions as given by Eq. (8) may be too high.
2. The empirically derived dependence of E^* upon T_A and h given in Eq. (8) does not take into account the phase P_{ag} of T_A relative to R_n and, consequently, it produces a seasonal phase error in the calculated potential evapotranspiration (cf. Fig. 5).
3. As already mentioned, by distributing the observed monthly precipitation equally over all of the days in the month, we overestimate the interception-loss E_I.
4. The empirically derived regression $E^*(R_A, h)$ was obtained from grass cover lysimeter measurements and from river runoff measurements in the grass covered and forested regions of the central and eastern USA where the surface of the vegetation is typically wet for only a small part of the year. But in forested regions where the surface is wet with rain a large part of the time, and especially if the winds are strong, the regression given by Eq. (8) may produce a significant underestimate of the interception-loss and, therefore, a significant underestimate of total evapotranspiration and overestimate of runoff. (See, for example, Shuttleworth and Calder 1979, Mintz 1982).
5. In the high latitude soil moisture budget we do not take into account freezing of the soil. When soil is frozen there is almost no infiltration, and it does not matter whether the supply of water to the soil is an assumed wintertime rainfall or an actual spring time snowmelt. In both cases the water will be removed as surface runoff before the soil has thawed and before the infiltration and evapotranspiration can begin. When we neglect freezing of the soil we therefore overestimate the soil moisture and evapotranspiration, and we underestimate the annual runoff.

Validation of the results

The only quantitative evaluation of our results which was possible at this stage is the comparison of the annual runoff, accumulated from our results over the largest river basins, with the corresponding river flows as estimated from Baumgartner and Reichel (1975). Results are shown in Fig. 13 and in Table 2. What is plotted in Fig. 13 is the estimated evapotranspiration (from our model) against the annual catchment evapotranspiration, obtained over each river basin as the difference between the amount of precipitation received and the river flow. At low or middle latitudes there is a very good correspondance between the two estimates. This means that the mean coefficients used in our governing equations represent rather adequately the ensemble effect of the various vegetation types found in these large river basins. It is fair to note however, that this is by no way a validation of our results in semi-arid regions, where such large rivers are not present. At high latitudes, we underestimate the river flows in a systematic manner. As already stated this may be related to the reduction of the soil field capacity due to the freezing of the ground, which we do not take in account. A possible source of error in our results is also, of course, the quality of the precipitation data themselves and this is especially true for high latitude regions; as emphasized by recent comparisons of various new data sets (Legates and Willmott 1990, Hulme 1991) the snow precipitation may be badly measured through conventional raingauges, and systematically underestimated in some climatologies. The rain measurements may also be in error over mountain areas.

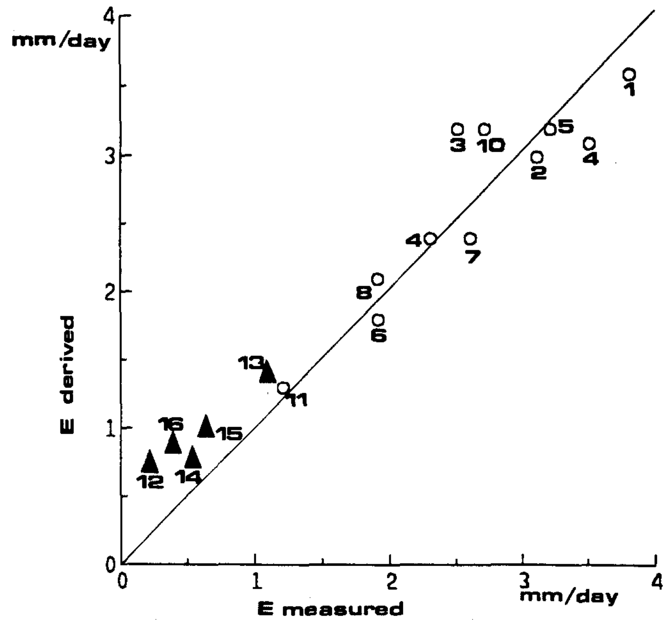

Fig. 13. Derived annual evapotranspiration (mm/day) versus measured annual catchment evapotranspiration (mm/day) from Baumgartner and Reichel (1975; Table 16). Numbers *1* to *16* indicate large river catchment basins as shown in Table 2. *Circles* (O) correspond to all river basins except at high latitudes; *triangles* (▲) indicate that the soil is frozen over most of the catchment during a large part of the year

Other indirect validation studies seem promising. It is, for example, possible (Serafini 1986) to use the number of months in which the soil wetness (ratio of W to W^*) is larger than 0.1 as an indicator of the natural vegetation. In particular, a good correlation was found between regions of natural forests and regions where this number of months was equal to 12. Also, qualitative comparisons have revealed a close correlation between the satellite-derived vegetation index (Tucker et al. 1986)

Table 2. Annual mean water budget of large river catchment basins

Basin	D $10^9\ m^3\ yr^{-1}$	A $10^6\ km^2$	$\tilde{D}$ mmday^{-1}	$\tilde{P}$ mmday^{-1}	$\tilde{E}_m$ mmday^{-1}	$\tilde{E}_d$ mmday^{-1}
1. Amazon	5992	7180	2.3	6.1	3.8	3.6
2. Congo	1325	3822	0.9	4.0	3.1	3.0
3. Orinoco	915	1086	2.3	4.8	2.5	3.2
4. Mekong	501	795	1.7	5.2	3.5	3.1
5. Irrawaddy	442	431	2.8	6.0	3.2	3.2
6. Ganges	489	1073	1.2	3.1	1.9	1.8
7. La Plata	615	2650	0.6	3.2	2.6	2.4
8. Brahmaputra	631	589	2.9	4.8	1.9	2.1
9. Yangtze-kiang	1104	1970	1.5	3.8	2.3	2.4
10. Sikiang	363	435	2.3	5.0	2.7	3.2
11. Mississippi	558	3224	0.5	1.7	1.2	1.3
12. St. Lawrence ▲	328	1030	0.8	1.0	0.2	0.8
13. Amur ▲	347	1843	0.5	1.6	1.1	1.4
14. Ob ▲	394	2950	0.4	0.9	0.5	0.8
15. Yenisei ▲	561	2599	0.6	1.2	0.6	1.0
16. Lena ▲	514	2430	0.6	1.0	0.4	0.9

where D is measured annual river flow, A is area of the catchment, $\tilde{D}=(D/A)$ or catchment area averaged measured annual river flow, $\tilde{P}$ is catchment area averaged measured annual precipitation, $\tilde{E}_m=(\tilde{P}-\tilde{D})$ is measured annual catchment evapotranspiration, $\tilde{E}_d$ is derived annual catchment evapotranspiration. ▲ indicates that the soil is frozen over most of the catchment during a large part of the year

and our ratio of actual to potential evapotranspiration. Finally the difference between the air temperature and the satellite radiative temperature gave a distribution very similar to our evapotranspiration distribution (Stowe et al. 1988, Fig. 6).

Conclusion

We have used a simple water budget model to derive monthly climatologies of the evapotranspiration and soil moisture distribution. Our method uses as input the long-term climatologies for precipitation and surface air temperature over the continents; these parameters are easy to measure at meteorological stations and there exist very long records of them, collected and processed by the various national weather services.

We have discussed quite extensively the assumptions made in deriving the model; it is clear that further progress is needed and that the same water budget experiments should be made with more detailed models that take into account more explicitly the role of the vegetation. As they stand, however, the distributions obtained in this paper are a useful first guess against which to compare further estimates, and may be of use in the validation of climate models, as for example shown by Gates et al. (1990) in the IPCC report.

Acknowledgements. The authors thank Dr H. Le Treut of Laboratoire de Météorologie Dynamique and Drs. M. Halem, E. Kalnay and Y. Sud of NASA/Goddard Space Flight Center, Laboratory for Atmospheres, for their interest and support of this work. They also thank G. K. Walker and L. Rumburg for drawing the figures, and M. C. Roos-Cally and M. A. Wells for typing the manuscript. Y. V. Serafini was a National Academy of Sciences/National Research Council Resident Research Associate at NASA/Goddard Space Flight Center when the work on this study was begun. Support to the University of Maryland for this research was provided by the U.S. National Science Foundation (Grant AMT-8309767) and the National Aeronautics and Space Administration (Grant NAG5-383).

References

Baumgartner A, Reichel E (1975) The world water balance: mean annual global, continental and maritime precipitation, evaporation and runoff. Elsevier, Amsterdam

Brankovic C, Van Maanen J (1985) The ECMWF climate system. ECMWF Tech Memo 109

Brutsaert W (1982) Evaporation into the atmosphere. Reidel Dordrecht/Boston/London

Budyko MI (ed) (1963) Atlas of the heat balance of the Earth. With NA Efimova: maps of the radiation balance for the continents. Main Geophysical Observatory, Leningrad CIS

Charney JG, Quirk W, Chow S, Kornfield S (1977) A comparative study of the effects of albedo change on drought in semiarid regions. J Atmos Sci 34:1366–1385

Davies JA, Allen CD (1973) Equilibrium, potential and actual evaporation from cropped surfaces in southern Ontario. J Appl Meteor 12:649–657

Gates WL, Rowntree PR, Zeng QC (1990) Validation of Climate Models in Climate Change: the IPCC Saentific Assessment Cambridge. University Press, Cambridge, 362 pp

Halstead MH (1954) The fluxes of momentum, heat and water vapor in micrometeorology. In: Micrometeoroloy of the surface layer of the atmosphere. Publications in climatology, The Johns Hopkins University, Laboratory of Climatology, USA 7 (1):233–361

Hillel D (1977) Computer simulation of soil-water dynamics: a compendium of recent work. International Development Research Centre, Ottawa, Canada

Hulme M (1991) An intercomparison of model and observed global precipitation climatologies. Geophys Res Lett 18:1715–1718

Hylckama TEA van (1956) The water balance of the Earth. Publications in climatology, 9

Jaeger L (1976) Monatskarten des Niederschlags fur die ganze Erde. Berichte Deutschen Wetterdienst 18 Nr 139, Offenbach, Germany

Legates DR, Willmott CJ (1990) Mean seasonal and spatial variability in gauge-corrected, global precipitation. Int J Clim 10:111-128

Lettau H, Davidson B (1957) Exploring the atmosphere's first mile, 2 Vols. Pergamon, Oxford New York

Louie PY, Pugsley WI (1981) Application of near realtime water budgets in monitoring climate-related events. Proceedings of the Fifth Annual climate diagnostic workshop, Univ of Washington, Seattle, 22-24 October 1980, National Oceanic and Atmospheric Administration, US Dept Commerce, pp 158-166

Mather JR (1962-1965) Average climatic water balance date of the continents. Part 1: Africa, Vol 15 (2), 1962; Part 2: Asia (excluding the USSR), Vol 16 (1), 1963; Part 3: USSR, Vol 16 (2) 1963; Part 4: Australia New Zeland and Oceania, Vol 16 (3) 1963; Part 5: Europe, Vol 17 (1), 1964; Part 6: North America (excluding the US), Vol 17 (2), 1964; Part 7: United States, Vol 17 (3), 1964; Part 8: South America, Vol 18 (2) 1965. Publications in Climatology. The Johns Hopkins University, Laboratory of Climatology. NJ, USA

Mather JR (1974) Climatology: fundamentals and applications. McGraw-Hill, New York

McGuiness JL, Bordne EF (1972) A comparison of lysimeter-derived potential evapotranspiration with computed values. Agricultural Research Service, Technical Bulletin No 1452, US Dept Agr, Washington DC, USA

McNaughton KG, Black TA (1973) A study of evapotranspiration from a Douglas fir forest using the energy balance approach. Water Resour Res 9:1579-1590

Miller DH (1977) Water at the surface of the Earth. Academic Press, New York USA

Mintz Y (1982) Influence of the vegetation structure on the thermal forcing of the atmosphere. Proceedings of the JSC Study Conference on the Physical Basis for Climate Prediction on Seasonal, Annual and Decadal Time Scales, Leningrad 13-17 September 1982

Mintz Y (1984) The sensitivity of numerically simulated climates to land-surface conditions. In: Houghton J (ed) The Global climate Cambridge University Press, pp 79-105

Mintz Y, Serafini Y (1981) Global fields of soil moisture and land-surface evapotranspiration. NASA Goddard Flight Center Tech Memo 83907, Research Review - 1980/81, 178-180

Mintz Y, Sellers PJ (1986) Proposal for a numerical model of the biosphere for use with numerical models of the atmosphere. In: Balakrishnan AV, Dorodnitsyn AA, Lions JL (eds) Vistas in applied mathematics. Springer New-York Berlin Heidelberg Tokyo, Ch 14, pp 244-264

Mintz Y, Serafini YV (1989) Global monthly climatology of soil moisture and water balance. LMD Internal Report No 148, Laboratoire de Météorologie Dynamique, Paris, France

Miyakoda K, Hembree GD, Strickler RP (1979) Cumulative results of extended forecast experiments. II: model performance for summer cases. Mon Wea Rev 197:395-420

Mustonen SE, McGuiness JL (1968) Estimating evapotranspiration in a humid region. USDA Agricultural Research Serivce. Technical Bulletin No 1389, US Dept Agr, Washington DC, USA

Nappo CJ (1975) Parameterization of surface moisture and evaporation rate in a planetary boundary layer model. J Appl Meteor 14:289-296

Palmer WC (1965) Meteorological drought. Res Paper 45, US Weather Bureau, US Dept Commerce, USA

Palmer WC (1968) Keeping track of crop moisture conditions nationwide: the new moisture index. Weatherwise 21:156-161

Penman HL (1948) Natural evaporation from open water, bare soil and grass. Proc R Soc (A) 193:120-145

Priestley CHB, Taylor RJ (1972) On the assessment of surface heat flux and evaporation using large-scale parameters. Mon Wea Rev 100:81-92

Randall DA (1983) Monthly and seasonal simulations with the GLAS climate model. Proc of the Workshop on Intercomparison of Large Scale Models Used for Extended Range Forecasts, European Centre for Medium Range Weather Forecasts, Reading, United Kingdom, pp 107-166

Ritchie JT, Burnett E, Henderson RC (1972) Dry land evaporative flux in a subhumid climate III. Soil water influence. Agronomy J 64:168-173

Rode AA (1969) Fundamental studies in hydrology. Part II: Methods of study of water regimes (in Russian). Gidrometeorologischeskow Izdatel stvo, Leningrad, CIS

Rutter AJ (1975) The hydrological cycle in vegetation. In: Monteith JL (ed) Vegetation and the atmosphere, Vol 1. Academic Press, London New York San Francisco, Ch 4, pp 111-154

Sellers PJ, Mintz Y, Sud YC, Dalcher A (1986) A simple biosphere model (SiB) for use within general circulation models. J Atmos Sci 43:505-531

Serafini YV (1986) Modélisation de l'interface sol-atmosphère en utilisant des données conventionnelles et satellitaires: impact climatique à grande échelle. Thèse de Doctorat d'Etat, Université de Paris VI (partly in English)

Serafini YV, Sud Y (1987) The time scale of the soils hydrology using a simple water budget model. J Climatol 7:581-591

Shuttleworth WJ, Calder IR (1979) Has the Priestley-Taylor Equation any relevance to forest evaporation? J Appl Meteor 18:639-646

Smith K, Ruhe A (1955) Water yearbook of agriculture. US Printing Office, Washington DC, USA

Spangler WML, Jenne RL (1984) Reference manual: world monthly surface station climatology. National Center for Atmospheric Research, Boulder, Colorado, USA

Stone PH, Chow S, Quirk WI (1977) July climate and a comparison of the January and July climates simulated by the GISS general circulation model. Mon Wea Rev 105:170-194

Stowe LL, Wellemeyer CG, Eck TF, Yeh HYM, Nimbus-7 Cloud data processing team (1988) Nimbus-7 global cloud climatology. Part I: algorithms and validation. J Climate 1:445-470

Strahler AN, Strahler AH (1978) Modern physical geography. Wiley, New York, USA

Suarez MJ, Arakawa A, Randall DA (1983) The parameterization of the planetary boundary layer in the UCLA general circulation model: formulation and results. Mon Wea Rev 111:2224-2243

Thornthwaite CW (1948) An approach toward a rational classification of climate. Geogr Rev 38:55-94

Thornthwaite CW (1954) A re-examination of the concepts and measurement of potential evapotranspiration. Publications in climatology, The Johns Hopkins University, Laboratory of Climatology, 7(1):200-209

Thornthwaite CW, Hare FK (1965) The loss of water to the air. Meteorol Monogr 28:163-180

Thornthwaite CW, Mather JR (1955) The water balance. Publications in climatology, The Johns Hopkins University, Laboratory of Climatology 9(2):59-117

Tucker CJ, Fung IY, Keeling CD, Gammon RH (1986) Relationship between atmospheric CO_2 variations and a satellite-derived vegetation index. Nature 319:195-199

Ward RC (1975) Principles of hydrology. 2nd ed. McGraw Hill, London New York

Willmott CJ, Rowe CM, Mintz Y (1985) Climatology of the terrestrial seasonal water cycle. J Climatol 5:589-606

Zubenok LI (1965) World maps of evaporativity. Sov Hydrl, pp 274-289 (English translation by S Molansky from Tr Glav Geofiz Obs, 179, 144-160)